Confinement of Polar Solvents within β-Cyclodextrins

Javier Rodriguez, Daniel Hernán Rico, Luis Domenianni, and Daniel Laria*

Departamento de Química Inorgánica, Analítica y Química-Física e INQUIMAE, Facultad de Ciencias Exactas y Naturales, Universidad de Buenos Aires, Ciudad Universitaria, Pabellón II, 1428, Buenos Aires, Argentina, and Departamento de Física, Comisión Nacional de Energía Atómica, Avenida Libertador 8250, 1429, Buenos Aires, Argentina

Using molecular dynamics techniques, we examined equilibrium and dynamical characteristics pertaining to the solvation of a single β-cyclodextrin (CD) in water and in dimethylsulfoxide (DMSO). Compared to its global minimum structure, the overall shape of the solute in solution is reasonably well preserved. While in aqueous solutions, the average number of solvent molecules retained within the central cavity of the oligosaccharide is close to 5, for DMSO, that number reduces to ∼1. No evidence of significant orientational correlations of the trapped molecules were found in either solvent. The main contributions to the hydrogen-bond (HB) connectivity between the solute and the bulk phases are due to the more distal HO6−O6 hydroxyl groups, acting as HB donors and acceptors. The average residence time for retained DMSO was found to be in the nanosecond range, and it is, at least, 1 order of magnitude longer that the one observed for water. We also analyzed the characteristics of the solvation of the β-CD in an equimolar water−DMSO mixture. In this environment, we found a preferential localization of a single DMSO molecule in the interior of the CD and a very minor retention of water. In the mixture, the characteristic time of residence of the trapped DMSO molecule increases by a factor of ∼2. The observed difference was rationalized in terms of the fluctuations of the local concentrations of the two species in the vicinity of the CD top and bottom rims.

I. Introduction

Cyclodextrins (CD) are oligosaccharides comprising several glucose units, linked in a toroidal structure by α-(1–4) glycosidic bonds.[1] Their usual denomination, based on Greek letter prefixes, refers to the number of glucose constituents (α: 6, β: 7, γ: 8, and δ: 9), although structures of macrocycles containing up to 48 units have also been reported.[2] Their overall molecular shape is normally portrayed in terms of a truncated cone, surrounding a central cavity ∼7−8 Å in height and diameters ranging from 4.5 up to 8 Å.

In recent years, there has been a growing interest in understanding the solvation of CD in aqueous media due to their applications as versatile complexing agents of small organic molecules, which are incorporated in their hydrophobic cavities.[3,4] The structural and dynamical features of CD in solution are the result of a complex interplay between thermal fluctuations and the characteristics of the coupling with the nearest solvation shells. Given the large variety of relevant lengthscales describing the structure of these complexes and the equally diverse nature of local interactions prevailing between different portions of the CD and the solvent molecules, one can anticipate complex scenarios, whose appropriate descriptions require a large extent of microscopic detail.

In a broader context, assessing the properties of water confined within the central cavity of a CD is akin to a more general class of phenomena, dealing with water in restrictive environments. The subject is of primary interest in biological sciences since many reactive processes, such as drug delivery,[5−7] molecular recognition,[8] and protein dynamics,[9] involve water molecules subjected to different degrees of confinement. Moreover, the term biological water has recently been coined to designate water molecules whose dynamical modes are partially hindered due to geometrical restrictions imposed by their closest environments. As a result, the range of the characteristic timescales describing the dynamical modes of these aqueous phases may stretch from the subpicosecond up to the nanosecond time domain or even longer.[10−12]

In a couple of recent papers, Shikata et al.[13,14] have analyzed dynamic aspects related to CD dissolved in water and dimethylsulfoxide (DMSO). For the specific case of DMSO, their results for the real and imaginary parts of the frequency dependent permittivity indicate that the average exchange times for DMSO molecules in close contact with the solute—albeit not trapped—were in the order of τ_{exch} ∼130−180 ps.[13] Moreover, by comparing the dynamical characteristics of the dielectric responses in a series CD with variable degree of methylation, they also concluded that the residence time of the trapped molecules would be similar to the one for those lying in contact with the more external portions of the CD. More recently, similar experiments performed in water have indicated that the corresponding timescales are approximately 1 order of magnitude shorter: τ_{exch} ∼ 20−30 ps.[14] In both cases, these dynamical modes would be controlled by the hydrogen bond (HB) dynamics between the hydroxyl groups of the solute and the different acceptor and donor sites in the solvents.

The present paper is largely motivated by these previous studies. In what follows, we will present results from extensive molecular dynamics experiments performed on systems composed of a single β-CD (7 glucose units, see Figure 1a) in water and in DMSO. In addition, and in order to analyze possible effects arising from preferential solvation, we also performed additional runs in which the CD was dissolved in a water−DMSO equimolar mixture. In the past, several experimental[15−22] and theoretical[20,23−29] studies addressed the analysis of the structure
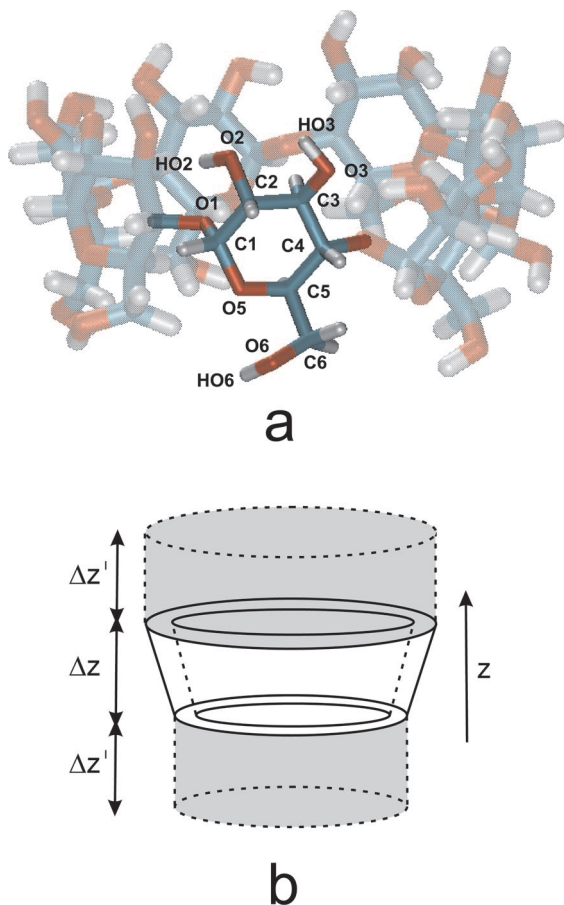
* Corresponding author. E-mail: dhlaria@cnea.gov.ar.

Figure 1. (a) β-CD. (b) Vertical windows for samplings within the interior (Δz) and the upper- and lower-rim regions ($\Delta z'$) of the β-CD.

and dynamics of CD in vacuo, in crystal phases, and in solution. Moreover, a sizable part of the research in this area is also devoted to the analysis of encapsulation phenomena of a wide variety of guest molecules. The general picture that emerges from the joint analysis of the large body of available experimental and theoretical work reveals that, despite the efforts, it is still difficult to single out a force field that would yield a unified, satisfactory description of the energetics, the structure, and the dynamics of cycldextrins in the different environments mentioned above.[30–34] With this caveat in mind, and with our goal mainly focused on the description of the local solvent spatial and dynamical fluctuations in the vicinity of solvated CD, we present molecular dynamics results that extend previous simulation experiments in aqueous solution to nonaqueous environments and polar mixtures. In particular, we examine the gross features pertaining to the amount of solvent molecules that can be trapped within a midsize CD cavity, the average residence times of these molecules, and the characteristics of the local solvent density fields in the vicinity of the different hydroxyl groups of the CD.

The organization of the paper is as follows: In section II, we briefly describe the model and the simulation procedure. Results for the pure water and DMSO liquid phases are presented in section III. The next section is devoted to the analysis of CD in water–DMSO mixtures. The concluding remarks of the work are presented in section V.

II. Model

The simulation experiments were performed on systems containing a single β-CD and N_α (α = water, DMSO) polar solvent molecules. We investigated pure solvent phases (N_W = 1648; N_{DMSO} = 466) and mixtures as well ($N_W = N_{DMSO}$ = 348).

The dynamical trajectories corresponded to *NPT* simulation runs. Temperature and external pressure were controlled by Nosé–Hoover type thermostats and barostats[35] set at T = 298 K and 1 bar, respectively. At these thermodynamics conditions, the lengths of the simulation boxes were of the order of $L \sim 37$ Å. The NAMD package[36] was used to run the dynamics of the systems; the code Hamiltonian is based on the CHARMM22 force field.[37] Specific interactions involving the CD atomic sites were taken from ref 38. This Hamiltonian has been extensively implemented to model carbohydrates[39] and cyclodextrins as well.[20]

Water interactions were modeled by the TIP3P model,[40] whereas, for the DMSO molecules [(CH$_3$)$_2$SO], we employed the flexible version of the P2 Hamiltonian of Luzar and Chandler,[41] as implemented by Benjamin.[42] The latter model has proved to provide reasonable estimates for structural and dynamical properties of pure DMSO and its mixtures with water at all mole fractions.[41–43] Long-ranged, Coulomb interactions were treated using Ewald summation techniques, using a particle mesh procedure.[44]

The simulation procedure involved an initial equilibration run of 200 ps, during which only the solvent molecules were allowed to move, at temperatures close to T = 700 K. From then on, the systems were gradually cooled down to temperatures close to ambient conditions, by multiple rescalings of the atomic velocities during a time interval of 100 ps. Finally, we released the constraints on the CD sites, and the systems were equilibrated at T = 300 K, during a final equilibration run of 200 ps. Meaningful statistics were collected during time spans typically lasting 25 ns. In all experiments, no major differences were found in statistical averages collected along different uncorrelated temporal subintervals lasting 5 ns.

III. Pure Solvents

A. Equilibrium Properties. In order to facilitate the analysis of the spatial correlations in the close vicinity of the CD in solution, we found it convenient to define a local system of coordinates, with its origin located at the center of mass of the solute, and with the unit vectors $\hat{x}, \hat{y}, \hat{z}$ aligned along the directions of the instantaneous principal axes of its inertia tensor. The magnitude of the principal moments of inertia served to identify each axis, in such a way that $I_x < I_y < I_z$.

At the crudest level of description, the latter quantities also provide an idea of the degree of distortion of the overall geometrical shape of the CD molecule. More specifically, the consideration of the eccentricity form parameter defined as

$$\varepsilon = \sqrt{1 - \frac{a^2}{b^2}} \tag{1}$$

with

$$a^2 = \frac{I_z - (I_y - I_x)}{2}$$
$$b^2 = \frac{I_z + (I_y - I_x)}{2} \tag{2}$$

yields an estimate of the deviations from the circular geometry of the ring structure. For solvated CD, we found roughly similar values of ε, regardless of the solvent considered: $\varepsilon = 0.6 \pm 0.05$. This number reveals a moderate distortion of the central cavity of the β-CD (for all practical purposes, ε for the global minimum structure in vacuo can be taken as 1), whose structure

Polar Solvents in β-Cyclodextrins

J. Phys. Chem. B, Vol. xxx, No. xx, XXXX **C**

Figure 3. Probability densities of observing N trapped molecules within a β-CD: (a) pure W; (b) pure DMSO; (c) W in 50/50 mixtures; (d): DMSO in 50/50 mixtures.
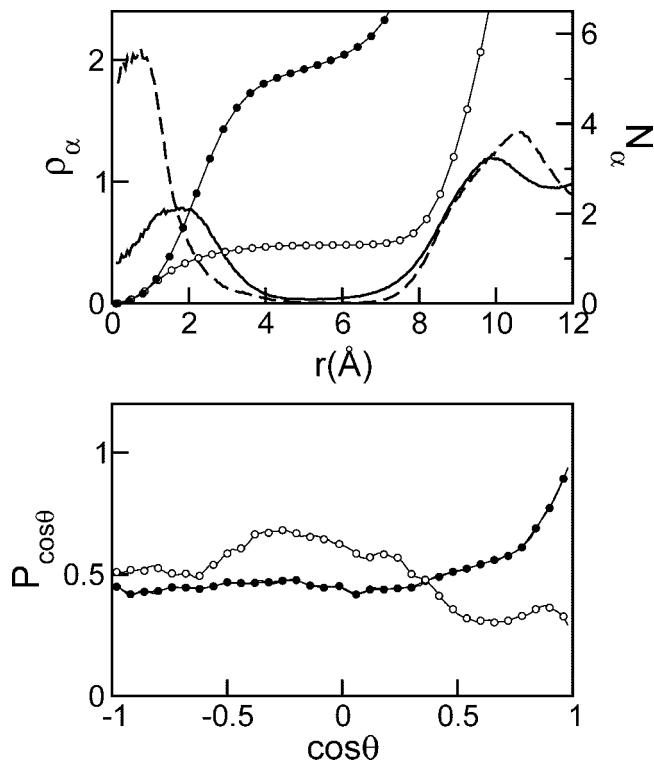
Figure 2. (top panel) Solvent density fields in the close vicinity of an infinitely diluted β-CD in W (solid lines, left axis) and DMSO (dashed line, left axis). Also displayed are results for the cumulative integrals for W (black circles, right axis) and DMSO (open circles, right axis). (bottom panel) Orientational distributions for trapped solvent molecules within β-CD: W (black circles), DMSO (open circles).

in solution can still be reasonably well described as a truncated cone, with a central cavity of radius $\sim$5 Å and a top-to-bottom-rim distance of roughly $d_{tb} \sim 7-8$ Å.

We now move to the analysis of the microscopic characteristics of the solvation of the β-CD. Perhaps the first and simplest question to be answered concerns the amount of solvent that can be confined within its central cavity. One can exploit the quasi-cylindrical symmetry of the molecule, to define solvent density fields of the type

$$\rho_\alpha(r) = \frac{1}{2\pi r \Delta z \bar{\rho}_\alpha} \left\langle \sum_i \delta(r_i^\alpha - r) H(z_i^\alpha) \right\rangle \qquad (3)$$

where $(x_i^\alpha, y_i^\alpha, z_i^\alpha)$ are the coordinates of ith site of type α, $r_i^\alpha = \sqrt{[(x_i^\alpha)^2 + (y_i^\alpha)^2]}$, and $\bar{\rho}_\alpha$ is the bulk density of site α. The characteristic function $H(z)$ is defined as 1 if $|z| < 3.5$ Å and 0 otherwise. Note that, with these definitions, the sampling at small values of r is restricted to the interior of the CD, i.e. a cylindrical volume of radius $r \sim 5$ Å and height $\Delta z = 7$ Å.

Results for the density fields of water ($\alpha = O_W$) and DMSO ($\alpha = S$) are shown in the top panel of Figure 2. The plots for both solvents present main central peaks located at $r <$ 4 Å which correspond to trapped molecules. There is also a 4 Å $\lesssim r \lesssim 7$ Å intermediate region where the solvent is excluded by the presence of the CD atoms and, finally, there is a third region with minor structure, extending beyond $r \sim$ 10 Å, which includes free solvent molecules in the close vicinity of the outer boundary of the solute. In passing, we remark that the choice for the window-width $\Delta z = 7$ Å corresponds to the maximum value that, after several tests, rendered $\rho_\alpha(r) \sim 0$ along the above-mentioned intermediate region (see Figure 1b).
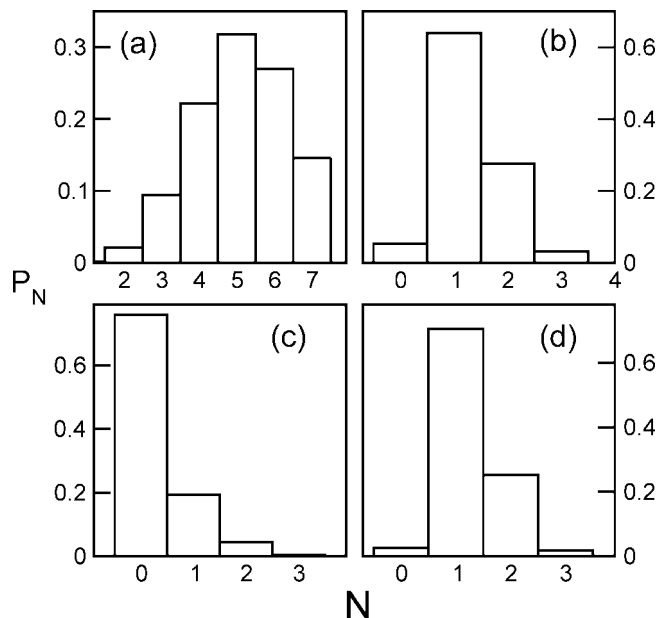
The areas under the main peaks

$$N_\alpha(r_o) = 2\pi \Delta z \int_0^{r_o} \rho_\alpha(r') r' \, dr' \qquad (4)$$

with $r_o \sim 5$ Å correspond to the number of confined solvent molecules. In agreement with previous studies,[45,46] we found that for water $N_W \sim 5$; whereas for DMSO, that number falls to approximately $N_{DMSO} \sim 1$ (see also top panel of Figure 2).

Concerning population fluctuations, in Figure 3, we present the histograms illustrating the corresponding probability densities for the number of trapped solvent molecules. For water, we observe that the distribution ranges from $\sim$3 up to 7 molecules, while for DMSO, there is a non-negligible, 30% chance of observing two molecules simultaneously trapped inside the CD.

In Figure 4, we show typical snapshots illustrating some common scenarios of trapped molecules. At a first glance, the inner waters in the top figure look like a handful of molecules, connected via a zigzag of hydrogen bonds. The middle and bottom panels show two configurations with trapped DMSO molecules lying closer to the top (Figure 4b) and bottom rims (Figure 4c), respectively. A more careful analysis of the average positions of these molecules, reveals a tendency for locations near the upper—and somewhat more open—rim of the CD. Note that in both cases, the O_{DMSO} site appears exposed to the bulk solvent. Given the characteristics of the previous descriptions and considering the specific charge distributions in both solvents, it is also of interest to investigate about possible orientational correlations of the trapped molecules. In the bottom panel of Figure 2, we present results for probability densities of the type

$$P_{\cos\theta} \propto \langle \delta(\cos\theta_i^\alpha - \cos\theta) \rangle_{trp} \qquad (5)$$

where

$$\cos\theta_i^\alpha = \frac{\hat{\mathbf{z}} \cdot \boldsymbol{\mu}_i^\alpha}{|\boldsymbol{\mu}_i^\alpha|} \qquad (6)$$

in the previous equations, μ_i^α represents the dipole of the ith molecule of type α ($\alpha = $ W, D). We stress that in eq 5, $\langle \cdots \rangle_{trp}$
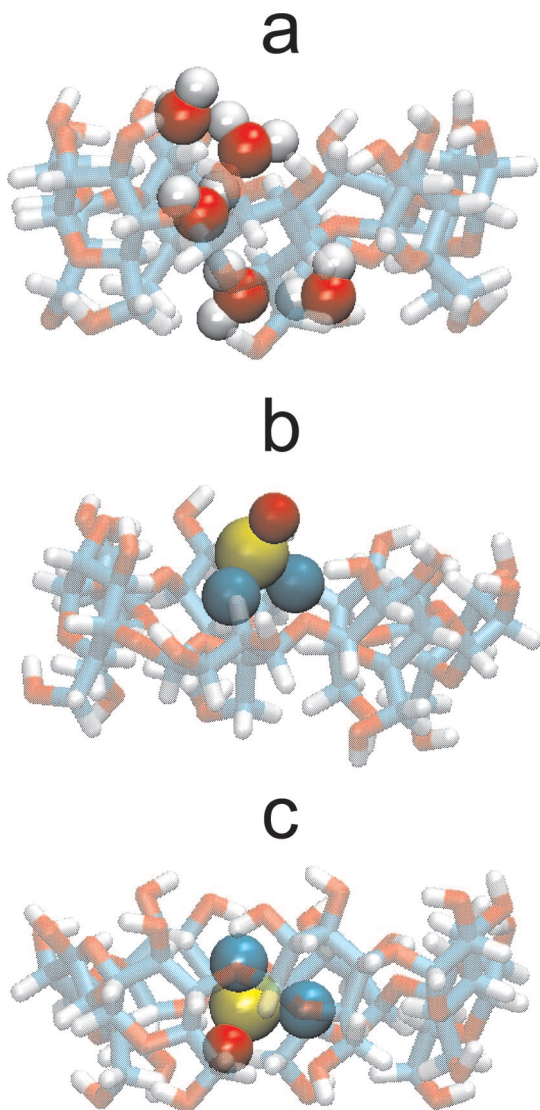
a

b

c

Figure 4. Snapshots of typical configurations of trapped solvent molecules within a β-CD cavity. (a) W; (b) DMSO (top rim); (c) DMSO (bottom rim).

denotes an ensemble average restricted to those molecules that lie within the interior of the CD. Both densities exhibit broad profiles with average values close to zero: $\langle \cos \theta_W \rangle_{trp} = 0.08$ and $\langle \cos \theta_{DMSO} \rangle_{trp} = -0.08$. Note that the presence of broad distributions is consistent with the features of the snapshots already mentioned above: on the one hand, a stringlike structure of hydrogen-bonded water molecules along the z direction with dipolar projections of alternating signs and, on the other, two external localizations, in the vicinity of the upper and lower rims, with opposite dipolar alignments.

Concerning spatial correlations between the CD and its closest environment, we focused attention on the HB connectivity between the OH groups in the solute and bulk molecules. In each glucose unit, there are three hydroxyl groups which can act as potential HB acceptor/donor groups: O6—HO6 (primary hydroxyls) and O2—HO2, O3—HO3 (both, usually referred to as secondary hydroxyls) (see Figure 1a). Although there are more accurate descriptions of HB connectivity based on geometrical and/or energetic criteria,[47] our analysis here was based on the areas under the main peaks of the site–site spatial correlations of the type

$$g_{\alpha\gamma}(r) = \frac{1}{4\pi r^2 \bar{\rho}_\gamma} \left\langle \sum_i \delta(|\mathbf{r}_\alpha - \mathbf{r}_\gamma^i| - r) \right\rangle \qquad (7)$$

where r_α identifies the coordinate of a solute site of type α (α = O2, O3, O6, HO2, HO3, HO6) and r_γ^i represents the coordinate of the ith site of type γ (γ = O_W, H_W, O_{DMSO}). Pyranoid (O5) and glycosidic (O4) oxygen sites also participate as acceptors of HB; however, previous studies have confirmed that, compared to the hydroxyl groups, the HB connectivity promoted via these sites is much less marked.[24,25,29]

Results for the site–site correlations are displayed in the three panels of Figure 5. In the bottom one, the profiles illustrate the HB acceptor characteristics of the β-CD hydroxyls in water. The three plots are characterized by main peaks located at $r =$ 2 Å and include an average of ∼1 HB (for O3 and O6) and 0.8 HB (for O2). As expected, the inhomogeneities in the solvent density fields provoked by the presence of different solute groups extend over lengthscales which are comparable to the diameter of the ring (in all cases, the $g(r)$ profiles differ from unity even beyond 10 Å).[48] Complementary information about the HB donor characteristics of the CD in water and in DMSO can be extracted from the main peaks of the profiles displayed in the middle and top panels, respectively. In both cases, the numbers of HB established by the three different OH groups, n_α, follow similar trends: $n_{HO3} < n_{HO2} < n_{HO6}$. For water, the average values are 0.2, 0.45, and 0.55 HB, while the corresponding areas for DMSO include 0.07, 0.3, and 0.75 HB. The magnitudes of the peaks indicate the clear preeminence of the HO6—O6 groups as the ones with more marked HB donor and acceptor characters.
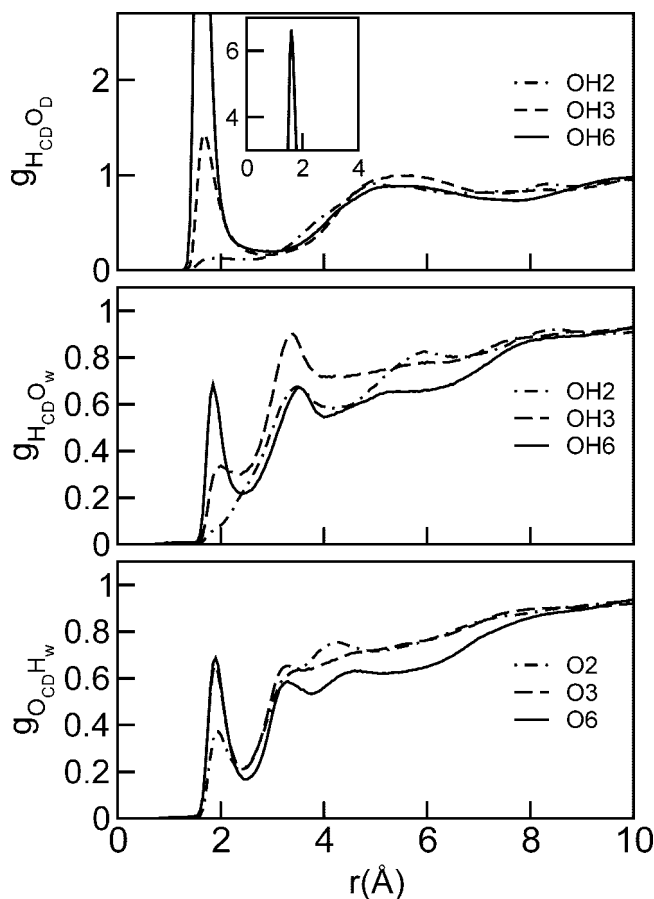

Figure 5. Pair correlation functions involving hydroxyl groups in β-CD and different solvent sites. Results shown in the bottom and central panels correspond to aqueous media; results shown in the top panel correspond to the pure DMSO phase.
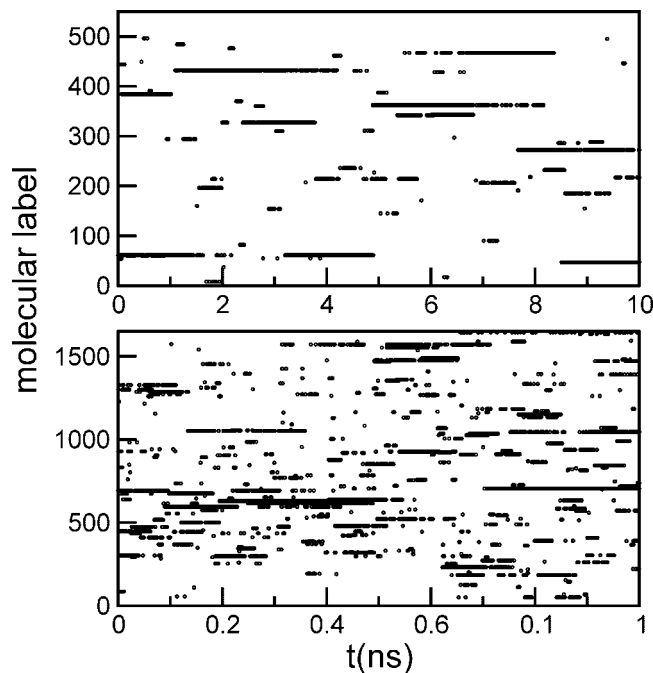
Polar Solvents in β-Cyclodextrins

J. Phys. Chem. B, Vol. xxx, No. xx, XXXX **E**

Figure 6. Solvent indexes corresponding trapped molecules within a β-CD. (top panel) DMSO. (bottom panel) W. Note the difference in the scales of the temporal axes.
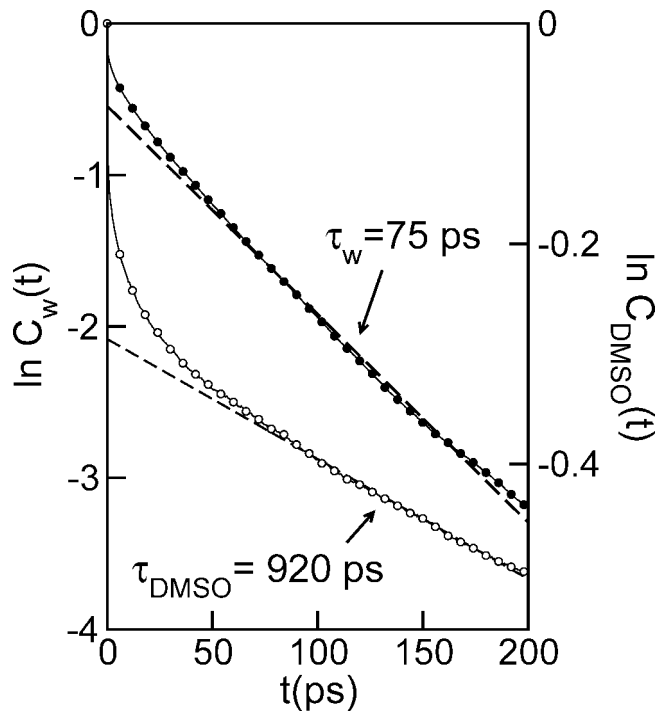

Figure 7. Time correlation functions for characteristic functions of trapped solvent molecules (see text). W black circles; DMSO open circles.

This observation can be simply rationalized invoking their somewhat more exposed spatial localizations within the molecule, a fact that would facilitate an easier approach of the solvent sites acting as potential HB donor/acceptor groups. Incidentally, the presence of practically no HB of the type $O_W \cdots HO2-O2$ or $O_{DMSO} \cdots HO2-O2$ led us to further investigate into the characteristics of the connectivity in the vicinity of these OH groups. The inspection of a large number of configurations revealed that the low intermolecular connectivity was in fact originated in an apparently much more stable, collective connectivity pattern of intramolecular HB of the type $O3' \cdots HO2-O2$. This is a very well-known feature that has been documented in the past.[19,27,45,49]

B. Dynamical Properties. The first dynamical aspect that we will analyze in connection with polar solvent confinement within CD concerns the average residence times for molecules located in its interior. The most direct route to get rough estimates of these quantities is by the inspection of the plots shown in Figure 6. In that figure, we display the time evolution of the indexes of trapped molecules. By simply examining the lengths of the horizontal segments and the differences in the temporal scales between the two panels, it is clear that residence times of the trapped DMSO molecules range in the nanosecond time scale, and are at least 1 order of magnitude longer that the characteristic residence times observed in water.

Still, a more rigorous analysis can be performed by analyzing the population relaxation time correlation functions: Consider the following characteristic variable $h_i^\alpha(t)$, which is defined as unity if the ith molecule of type α lies within the CD interior at time t and 0 otherwise. The time correlation functions of interest are of the type

$$C_\alpha(t) = \frac{\langle \delta h_i^\alpha(t) \delta h_i^\alpha(0) \rangle}{\langle (\delta h_i^\alpha)^2 \rangle} \qquad (8)$$

where $\delta h_i^\alpha(t) = h_i^\alpha(t) - \langle h_i^\alpha \rangle$ represents the instantaneous fluctuation of the variable h_i^α away from its equilibrium value.

Normally, one can extract the inverse of the residence time τ_α^{-1} from the linear decay of $\ln C_\alpha(t)$ at long time spans.

Results for the population relaxations for water and DMSO appear in Figure 7. After transient time intervals intermediate between 25 and 100 ps, both curves exhibit single-exponential decays, with characteristic timescales of ~75 ps for water and ~1 ns for DMSO. Given the total temporal length of our experiments (of the order of 30 ns), the latter estimate is likely to be affected by some non-negligible uncertainty. Anyhow, the results corroborate that trapped DMSO molecules remain within these CD a time interval that is, at least, 1 order of magnitude longer than the one observed for a water molecule. Moreover, the residence time is significantly longer than the experimental result of the average time for the exchange process of DMSO molecules in the first solvation shell $\tau_{ex} = 130$ ps.[13]

The fact that characteristic times associated to DMSO dynamical variables are longer than their counterparts observed in water is somehow expected: Diffusion coefficients and rotation characteristic times are only a couple of important examples where these trends are experimentally found in the corresponding bulk phases. Consequently, one could invoke these differences in the dynamical characteristics of the two liquids to explain—at least partially—the disparities between the trapping timescales. The physical interpretation of the individual values requires a dynamical analysis that certainly exceeds the objective of the present paper, so for the purposes of the present discussion, we will only briefly comment on some qualitative arguments that may prove to be helpful in future and more rigorous interpretations of the confining mechanisms. On the basis of the individual paths of the molecules, the gross features of the trapping processes can be classified into two categories: (i) We observed episodes in which the molecule gets trapped and released at the same rim of the CD. (ii) On the other hand—and specially for water—we also found trajectories that get across the internal cavity of the CD. In both cases, the characteristic lengthscale associated with these processes should
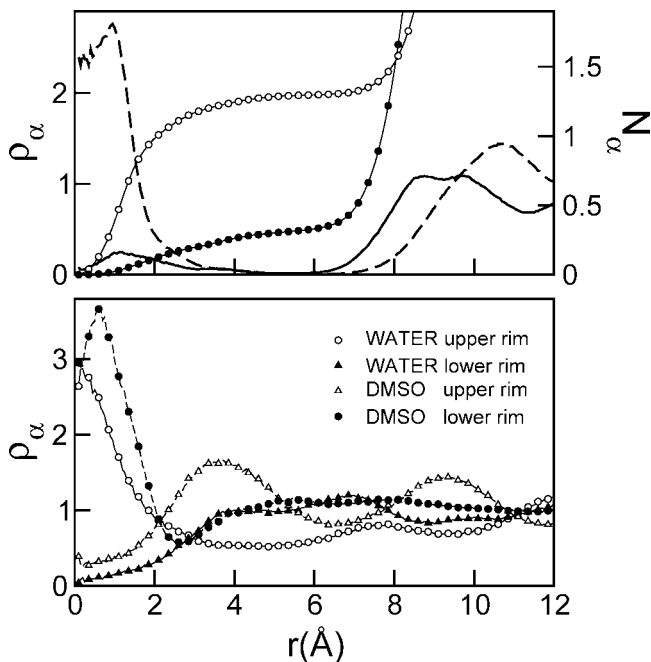
Figure 8. (top panel) Same as top panel of Figure 2 for an equimolar DMSO−W mixture. (bottom panel) Solvent density fields in the close vicinity of the bottom and top rims (see text) of an infinitely dilute β-CD in an equimolar DMSO−W mixture.

be comparable to Δz. Assuming a free diffusive path along the central cavity, the characteristic time of residence would be $\tau_w \sim (\Delta z)^2/2D_{TIP3P} \sim 40$ ps, where $D_{TIP3P} \sim 0.6$ Å^2 ps^{-1} corresponds to the diffusion coefficient of the water TIP3P model in the bulk.[50] As such, this observation would indicate differences in a factor of ~ 2 in the "effective" transport coefficient of water promoted by geometrical restrictions and specific interactions that prevail in the interior of the CD. For the DMSO case, the modifications operated in the dynamics of the trapped molecules are even more striking: note that the sole consideration of the reduction in the value of its diffusion constant[43]—$D_{DMSO} \sim D_{TIP3P}/6$—is insufficient to explain the differences in the residence times: $\tau_{DMSO} \sim 14\tau_w$. We can speculate on two reasons to account for this additional retardation: (i) more drastic steric restrictions preventing diffusive and rotational motions of a bulkier molecule within and through the CD central channel and (ii) an energetic stabilization of the DMSO molecule provided by hydrophobic forces prevailing at the CD interior. As such, both effects would act as "anchoring" agents for the retained DMSO molecule. As we mentioned above, the confirmation of these arguments await a more detailed analysis, so we will not proceed any further.

IV. Mixtures

In this section, we will analyze the characteristics of solvent trapping in water−DMSO equimolar mixtures. Following similar lines of analysis to those implemented for the pure solvent cases, in the top panel of Figure 8, we present results for the density fields in the interior of the CD. At a first glance, the plots look similar to those depicted in Figure 2; however, here, there seems to be a clear preferential trapping of DMSO. The cumulative integrals N_α (c.f. eq 4) level off at approximately 1.1 DMSO molecules, while, in practically 75% of the configurations, one finds no signs of confined water molecules. This observation seems to corroborate the conventionally accepted picture of the interiors of CD, which are usually portrayed as environments with a clear hydrophobic character.
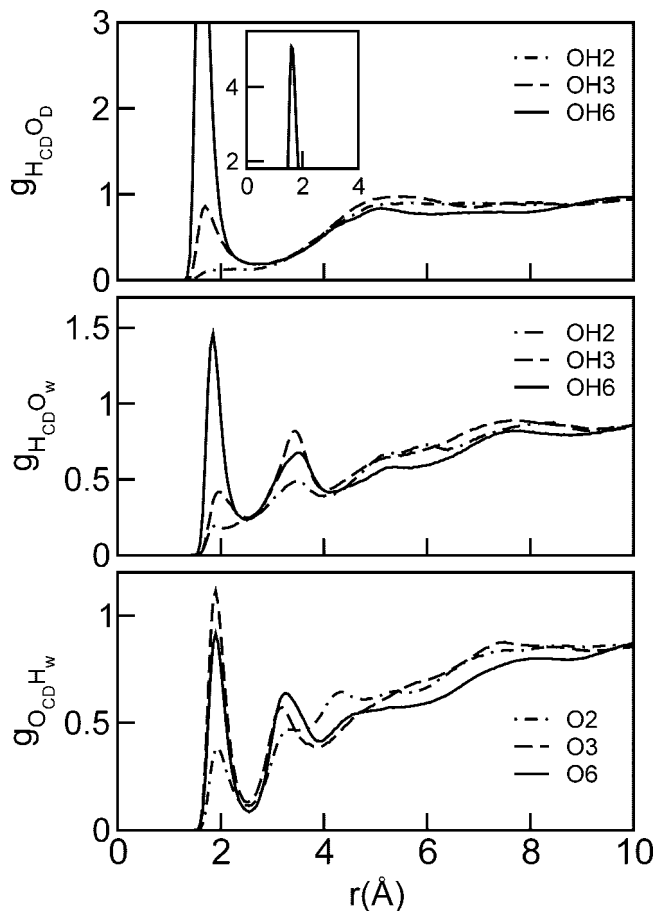

Figure 9. Same as Figure 5 for an equimolar W−DMSO mixture.

The HB connectivity of the CD hydroxyl groups is depicted in Figure 9 in terms of spherically symmetric site–site pair correlation functions. To facilitate a better interpretation of the confinement dynamics in mixtures, it will be convenient to discriminate hydrogen bonds based on their locations: on the one hand, contributions from secondary OH groups located in the upper rim; and on the other, contributions from primary groups located at the bottom rim. The HB acceptor characteristics of the CD are presented in the bottom panel: The areas under the main peaks include a total of 0.45 and 0.25 HB located at the upper and lower rims, respectively. Concerning the HB donor characteristics, the middle panel (W) shows a total of 0.2 HB of the type $H_2O\cdots HO6-O6$ and 0.1 HB of the type $H_2O\cdots HO3-O3$; finally, the main peaks of the curves in the top panel (DMSO) include 0.5 HB of the type $O_{DMSO}\cdots H6O6-O6$ and 0.2 HB of the type $O_{DMSO}\cdots HO3-O3$. Similarly to what is found in pure solvent cases, HB contributions from donor $HO2-O2$ groups are negligible. The general picture that emerges from these observations suggests that, in mixtures, the interior does not differ substantially from what is found in the pure DMSO case, while the overall HB connectivity between the CD and its closest environment is somewhat diminished.

From the dynamical side, the changes in residence times are much more marked. In Figure 10, we present results for the corresponding population relaxations. Compared to the pure solvent cases, the magnitude of τ_{DMSO} is approximately a factor of 2 longer, whereas for the single water molecules which eventually get trapped, their residence times go up to a factor of ~ 4. Note that the observation concerning the quality of our predictions—already mentioned when we analyzed the pure DMSO case—should be observed even more carefully in the
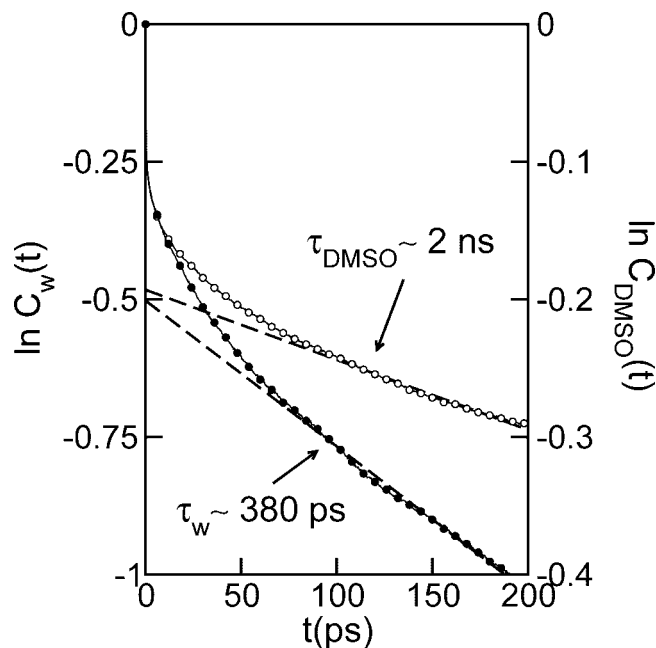
Polar Solvents in β-Cyclodextrins

J. Phys. Chem. B, Vol. xxx, No. xx, XXXX **G**

Figure 10. Same as Figure 7 for W−DMSO mixtures.

present situation; consequently, the magnitude of our estimates for τ should be regarded only as qualitative indicators.

Still, it is of interest to investigate the reasons for this additional retardation. Given that the interior of the CD in mixtures looks similar to the pure DMSO case, we focused attention on unveiling distinctive characteristics that may provide some clues in order to understand the observed dynamical differences. One can speculate on, at least, two major causes affecting the trapping dynamics: (i) On the one hand, the mechanism of ejection and subsequent incorporation of a trapped DMSO molecule might be controlled by some dynamical mode—involving either a general rearrangement in the CD or in the HB dynamics—which changes substantially as we compare the solvation in DMSO and in the water−DMSO mixture. (ii) On the other hand, it would also be possible that the external environments in the close vicinity of the CD may exhibit important modifications in the local densities of the species, affecting the residence times in a sensible fashion.

Concerning hypothesis i, the examination of many trajectories did not show clear signs of correlation between DMSO incorporation/ejection episodes and evident modifications in the overall shape of the CD and/or HB dynamics. In passing, we did corroborate that incorporations and ejections were mostly operated in a sequential fashion, an observation that is accordant with the information provided by the histogram d of Figure 3, which shows that the episodes where the CD remains empty occur only very rarely (∼1% of the configurations). Concerning hypothesis ii, the examination of local solvent concentration fluctuations in more external regions—close to the rims—did show important modifications. In the bottom panel of Figure 8, we present results for solvent density fields obtained from samplings restricted to two cylindrical volumes extending $\Delta z'$ = 7 Å above and below the original interior of the CD (see shaded areas in Figure 1b). Note that local concentration fluctuations at the top rim—the one with more room for the sequential incorporations and ejections of DMSO molecules— exhibit a clear concentration enhancement of water molecules. The opposite trend is found at the bottom rim. Moreover, these modifications go hand in hand with the extent of hydrogen bonding observed at the rims (c.f. Figure 5): the number of HB

established between each top-rim-OH group and water adds up to 0.45 + 0.2 = 0.6 (acceptor + donor); while for DMSO, that number is only 0.2 (donor). On the basis of entropic arguments, we are led to believe that the DMSO deficit at the top rim would restrain the replacement of the trapped molecules for a new, incoming one. Note also that, given the hydrophobic characteristics of the CD cavity, the replacement of the DMSO molecule for neighboring water would also be energetically unfavorable. Given this picture, we are led to believe that the joint consideration of these observations may provide plausible clues for a correct physical interpretation of the differences in τ_{DMSO} found in pure and mixed polar media.

V. Summary and Concluding Remarks

In this paper, we have presented new insights concerning the nature of solvent confinement in CD cavities. Two solvents have been examined: one protic (water) and a second, aprotic (DMSO). In addition to the corresponding pure phases, we also analyzed solvation in equimolar mixtures. Our results show that the amount of trapped water typically fluctuates between four and six molecules; whereas for DMSO, that number drops to practically ∼1. Note that these numbers roughly coincide with what one could expect based on the differences in the bulk densities—or equivalently, molecular sizes—of the two solvents at ambient conditions: $\rho_W/\rho_{DMSO} \sim 4$. This observation would indicate that, at least for β-CD, the number of trapped solvent molecules would be mainly controlled by packing effects and, to a lesser degree, by the hydrophobic characteristics of the cavity. Moreover for water, we did not observe local concentration fluctuations corresponding to configurations in which the cavity is devoid of molecules;[51] we tend to believe that the free energy costs for such fluctuations are prohibitively high. Although we did not undertake a rigorous quantitative analysis of the rotational motions inside the cavity, we found no evident signs of orientational order, a fact that might suggest only a moderate extent of rotational restrictions.

Concerning the intermolecular connectivity with the closest solvation shells, we focused attention on HB established by the hydroxyl groups located at the upper and lower rims of the CD. In all environments, we observed that the primary O6−HO6 hydroxyls play a preeminent role as HB donors and acceptors. In addition, we also corroborate the persistence of intramolecular hydrogen-bonding between adjacent glucose units of the type O3′···HO2−O2, a connectivity pattern that has been experimentally observed as well.[19,27,45,49]

From the dynamical side, perhaps the most important conclusion that can be drawn from our simulation experiments is the large disparity observed between the residence times of the trapped molecules: $\tau_{DMSO} \sim 1$ ns vs $\tau_W \sim 100$ ps. In this respect, our predictions clash with the interpretation of the results from time dependent permittivity experiments, that brings those timescales down to ∼200 and 30 ps, respectively. Yet, characteristic solvation timescales in the nanosecond temporal domain are not unusual in confined systems and have been reported in fluorescence experiments of confined Coumarins in CD.[52] As such, the source of the discrepancy is still elusive to us and will surely require further investigation.

The examination of water−DMSO mixtures revealed the following features: (i) As expected, due to its hydrophobic characteristics, the central cavity of the CD represents a more favorable solvation environment for DMSO than for water. (ii) More interesting is the connection that we established between concentration fluctuations of both species at the upper rim of the CD—the one exhibiting a wider diameter—and the exchange

dynamics. In particular, the joint effects of the depletion of DMSO molecules available for the exchange and the less favorable solvation of the more abundant water molecules would explain the retardations in the exchange processes between the trapped molecules in the CD cavity and the bulk.

There are many open questions concerning the structure and dynamics of CD in solution that still await proper elucidation. Among those intimately related to the results presented here, we can list the following: (i) In the course of our simulations, we observed global changes in the overall geometry of CD, promoted by rotations along intersaccharide dihedral angles. To what extent these rare events may affect the dynamics of the trapping processes is still unknown and worth examining. (ii) Cavity size and functionalization of the CD are certainly other important issues that will require attention. On the one hand, it will be interesting to assess whether the preferential solvation of DMSO still persists in larger cavities, such as those generated in γ- or δ-CD. On the other hand, the examination of CD with different degree of methylation will necessarily modify hydrogen-bonding. Should our interpretations remain valid, these changes, in turn, should also have dynamical implications on retention mechanisms. (iii) Also connected to the reactive channels that drive trapping and exchange processes in mixtures, a question that remains unanswered is why the presence of DMSO affects residence times for water, in approximately a factor of ∼4. (iv) Of course, a careful analysis on how sensitive the results presented in this paper are to the particular Hamiltonian choice would be desirable. Anyhow, we tend to believe that the qualitative conclusions that we have drawn from the present study—especially those pertaining differences between the two solvents investigated—should remain valid, regardless of the eventual modifications operated in the Hamiltonian employed to model intra- and intermolecular interactions involving the CD.

References and Notes

(1) For comprehensive information about cyclodextrins, see the special issue corresponding to the 98th volume of Chemical Reviews (1998).

(2) Ivanov, P. M.; Jaime, C. *J. Phys. Chem. B* **2004**, *108*, 6261.

(3) (a) Reija, B.; Wajih Al-Soufi, W.; Novo, M.; Tato, J. V. *J. Phys. Chem. B* **2005**, *109*, 1364. (b) Douhal, A. J. *Photochem. Photobiol. Part A: Chem.* **2005**, *173*, 229. (c) Okazaki, M.; Kuwata, K. *J. Phys. Chem.* **1984**, *88*, 4181.

(4) (a) Kano, K.; Kato, Y.; Kodera, N. *J. Chem. Soc., Perkin Trans.* **1996**, *2*, 1211. (b) Yu, Y.; Chipot, C.; Cai, W.; Shao, X. *J. Phys. Chem. B* **2006**, *110*, 6372. (c) Balabai, N.; Linton, B.; Napper, A.; Priyadarshy, S.; Sukharevsky, A. P.; Waldeck, D. H. *J. Phys. Chem. B* **1998**, *102*, 9617.

(5) Hyrayama, F.; Vekama, K. *Adv. Drug Deliver. Rev.* **1999**, *36*, 125.

(6) Uekama, K.; Hirayama, K.; Irie, T. *Chem. Rev.* **2002**, *98*, 2045.

(7) Szejtli, J. *J. Incl. Phenom.* **1991**, *14*, 25.

(8) (a) Kuwabara, T.; Kazuyo Shiba, K.; Ozawa, M.; Miyajima, N.; Yasutada, S. *Tetrahedron Lett.* **2006**, *47*, 4433. (b) Clark, J. L.; Peinado, J.; Stezowski, J. J.; Vold, R. L.; Huang, Y.; Hoatson, G. L. *J. Phys. Chem. B* **2006**, *110*, 26375. (c) Menuel, S.; Duval, R. E.; Cuc, D.; Mutzenhardt, P.; Alain Marsura, A. *New J. Chem.* **2007**, *31*, 995.

(9) Pizzitutti, F.; Marchi, M.; Sterpone, F.; Rossky, P. J. *J. Phys. Chem. B.* **2007**, *111*, 7584.

(10) Nandi, N.; Bagchi, B. *J. Phys. Chem. A* **1997**, *101*, 10954.

(11) Battacharyya, K.; Bagchi, B. *J. Phys. Chem. A* **2000**, *104*, 10603.

(12) Bhattacharyya, K. *Acc. Chem. Res.* **2003**, *36*, 95.

(13) Shikata, T.; Takahashi, R.; Onji, T.; Satokawa, Y.; Harada, A. *J. Phys. Chem. B.* **2006**, *110*, 18112.

(14) Shikata, T.; Takahashi, R.; Satokawa, Y. *J. Phys. Chem. B* **2007**, *111*, 12239.

(15) Vajda, S.; Jimenez, R.; Rosenthal, S. J.; Fidlert, V.; Fleming, G. R., Jr. *J. Chem. Soc. Faraday. Trans.* **1995**, *91*, 867.

(16) Bher, J. P.; Lehn, J. M. *J. Am. Chem. Soc.* **1976**, *98*, 1743.

(17) Douhal, A.; Fiebig, T.; Chachisvilis, M.; Zewail, A. H. *J. Phys. Chem. A* **1998**, *102*, 1657.

(18) Douhal, A. *Chem. Rev.* **2004**, *104*, 1955.

(19) Zabel, V.; Saenger, W.; Mason, S. A. *J. Am. Chem. Soc.* **1986**, *108*, 3664.

(20) Kevin, J.; Naidoo, K. J.; Chen, J. Y.-J.; Jansson, J. L. M.; Widmalm, G.; Maliniak, A. *J. Phys. Chem. B* **2004**, *108*, 4236.

(21) Scypinski, S.; Drake, J. M. *J. Phys. Chem.* **1985**, *89*, 2432.

(22) Sen, S.; Sukul, D.; Dutta, P.; Bhattacharyya, K. *J. Phys. Chem. A* **2001**, *105*, 10635.

(23) Lipkowitz, K. B. *Chem. Rev.* **1998**, *98*, 1829, and references therein.

(24) Manunzaa, B.; Deiana, S.; Pintore, M.; Gessab, C. *J. Mol. Struc. (Theochem)* **1997**, *419*, 133.

(25) Lawtrakul, L.; Viernstein, H.; Wolschann, P. *Int. J. Pharm.* **2003**, *256*, 33.

(26) Starikov, E. V.; Bräsicke, K.; Knapp, E. W.; Saenger, W. *Chem. Phys. Lett.* **2001**, *336*, 504.

(27) (a) Koehler, J. R. H.; Saenger, W.; van Gunsteren, W. F. *Eur. Biophys. J.* **1987**, *15*, 197. (b) Koehler, J. R. H.; Saenger, W.; van Gunsteren, W. F. *Eur. Biophys. J.* **1987**, *15*, 211. (c) Koehler, J. R. H.; Saenger, W.; van Gunsteren, W. F. *Eur. Biophys. J.* **1988**, *16*, 153. (d) Koehler, J. R. H.; Saenger, W.; van Gunsteren, W. F. *J. Mol. Biol.* **1988**, *203*, 241.

(28) Varady, J.; Wu, X.; Wang, S. *J. Phys. Chem. B* **2002**, *106*, 4863.

(29) Heine, T.; Dos Santos, H. F.; Patchkovski, S.; Duarte, H. A. *J. Phys. Chem. A* **2007**, *111*, 5648.

(30) For a critical review of the quality of different Hamiltonian models, see: Pérez, S.; Imberty, A.; Engelsen, S. B.; Gruza, J.; Mazeau, K.; Jimenez-Barbero, J.; Poveda, A.; Espinosa, J.-F.; van Eyck, B. P.; Johnson, G.; French, A. D.; Kouwijer, M. L. C. E.; Grootenius, P. D. J.; Bernardi, A.; Raimondi, L.; Senderowitz, H.; Durier, V.; Vergoten, G.; Rasmussen, K. *Carbohydr. Res.* **1998**, *314*, 141.

(31) (a) Englesen, S. B.; Pérez, S. *Carbohydr. Res.* **1996**, *292*, 21. (b) Engelsen, S. B.; Hervé-du-Penhoat, C.; Pérez, S. *J. Phys. Chem.* **1999**, *99*, 13334.

(32) Corzana, F.; Motawia, M. S.; Hervé-du-Penhoat, C.; Pérez, S.; Tschampel, S. M.; Woods, R. J.; Engelsen, S. B. *J. Comput. Chem.* **2004**, *25*, 573.

(33) French, A. D.; Johnson, G. P. *Carbohydr. Res.* **2007**, *342*, 1223.

(34) (a) Momany, G. A.; Willett, J. K. *Carbohydr. Res.* **2000**, *326*, 1994. (b) Momany, G. A.; Willett, J. K. *Carbohydr. Res.* **2000**, *326*, 210.

(35) (a) Martyna, G. J.; Tobias, D. J.; Klein, M. L. *J. Chem. Phys.* **1994**, *101*, 4177. (b) Feller, S. E.; Zhang, Y.; Pastor, R. W.; Brooks, B. R. *J. Chem. Phys.* **1995**, *103*, 4613.

(36) Phillips, J. C.; Braun, R.; Wang, W.; Gumbart, J.; Tajkhordshid, E.; Villa, E.; Chipot, C.; Skeel, R. D.; Kale, L.; Schulten, K. J. *Comput. Chem.* **2005**, *26*, 1781.

(37) MacKerell, A. D., Jr.; Bashford, D.; Bellott, R. L.; Dunbrack, R. L., Jr.; Evanseck, J. D.; Field, M. J.; Fischer, S.; Gao, J.; Guo, H.; Ha, S.; Joseph-McCarthy, D.; Kuchnir, L.; Kuczera, K.; Lau, F. T. K.; Mattos, C.; Michnick, S.; Ngo, T.; Nguyen, D. T.; Prodhom, B.; Reiher, W. E., III; Roux, B.; Schlenkrich, M.; Smith, J. C.; Stote, R.; Straub, J.; Watanabe, M.; Wiorkiewicz-Kuczera, J.; Yin, D.; Karplus, M. *J. Phys. Chem. B.* **1998**, *102*, 3586, and references therein.

(38) Kuttel, M.; Brady, J. W.; Naidoo, K. J. *J. Comput. Chem.* **2002**, *23*, 1236.

(39) Eklund, R.; Wildman, G. *Carb. Res.* **2003**, *338*, 393.

(40) Jorgensen, W. L.; Chandrasekhar, J.; Madura, J. D.; Impey, R. W.; Klein, M. L. *J. Chem. Phys.* **1983**, *79*, 926.

(41) Luzar, A.; Chandler, D. *J. Chem. Phys.* **1998**, *98*, 8160.

(42) Benjamin, I. *J. Chem. Phys.* **1999**, *110*, 8070.

(43) Senapati, S. *J. Chem. Phys.* **2002**, *117*, 1812.

(44) Yeh, I.-C.; Berkowitz, M. L. *J. Chem. Phys.* **1999**, *111*, 3155.

(45) (a) Betzel, C.; Saenger, W.; Hingerty, B. E.; Brown, G. M. *J. Am. Chem. Soc.* **1974**, *96*, 3630. (b) Raddaini, G.; Ganazzoli, F. *Chem. Phys.* **2007**, *333*, 128.

(46) In ref 29, the number of trapped water molecules was ∼7, although differences in the boundaries for the CD interior may account for the discrepancy.

(47) See Martí, J.; Padro, J. A.; Guàrdia, E. *J. Chem. Phys.* **1996**, *105*, 639, and references therein.

(48) We did verify that all radial distribution functions reach their assymptotic value $g_{\alpha\gamma}(r)$ ∼1 for $r = L/2$.

(49) See, for example: (a) Steiner, T.; Saenger, W. *Carb. Res.* **1994**, *259*, 1. (b) Klar, B.; Hingerty, B. E.; Saenger, W. *Acta Crystallogr. B* **1980**, *36*, 1154. (c) Koehler, J. E. H.; Saenger, W.; van Gunsteren, W. F. *J. Mol. Biol.* **1988**, *203*, 241. (d) Snor, W.; Liedl, E.; Weiss-Greiler, P.; Karpfen, A.; Viernstein, H.; Wolschann, P. *Chem. Phys. Lett.* **2007**, *441*, 159.

(50) Mark, P.; Nilsson, L. *J. Chem. Phys. A* **2001**, *105*, 9954.

(51) For drying transitions in nanocavities see, for example: Lum, K.; Chandler, D.; Weeks, J. D. *J. Phys. Chem. B* **1999**, *103*, 4570.

(52) Sen, P.; Roy, D.; Mondal, S. K.; Sahi, K.; Ghosh, S.; Bhattacharyya, K. *J. Phys. Chem. A* **2005**, *109*, 9716.